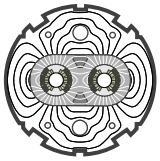

LHC Project Note 416

July 11, 2008

Werner.Herr@cern.ch

Results of dynamic aperture studies for increased β^* with beam-beam interactions

W. Herr, AB Department, CERN, 1211-Geneva 23
D. Kaltchev, TRIUMF, Vancouver, Canada

Keywords: dynamic aperture, beam-beam

Summary

We have evaluated the dynamic aperture in the presence of beam-beam effects for alternative running scenarios, in particular for the commissioning and early operation of the LHC. For top energy of 7 TeV we have studied the effect of increased β^* up to $\beta^* = 2$ m and found the expected increase of dynamic aperture for a moderate loss of luminosity. We have further studied the possibility of head-on collisions with a small number of bunches at injection energy.

1 Introduction

1.1 Parameter dependence of long range beam-beam interactions

The normalized beam separation in drift space between interaction point and first quadrupole is (for small β^*):

$$d = \frac{\alpha \cdot s}{\sigma(s)} = \frac{\alpha \cdot s}{\sqrt{\epsilon\beta(s)}} = \frac{\alpha \cdot s}{\sqrt{\epsilon(\beta^* + \frac{s^2}{\beta^*})}} \approx \frac{\alpha \cdot \sqrt{\beta^*}}{\sqrt{\epsilon}} \tag{1}$$

For the nominal parameters with the normalized emittance $\epsilon = 3.75$ μm, full crossing angle $\alpha = 2 \cdot 142.5$ μrad, and $\beta^* = 0.55$ m we get a normalized separation of approximately 9.4 σ in the drift space between the interaction point and the first quadrupole [1, 2]. Although most long range interactions occur within this drift space, i.e. at a constant separation, further long range encounters happen inside the focussing triplet. The normalized separation for those encounters changes depending on the optics and a few encounters at significantly smaller separation must be expected. For the nominal parameters the minimum separation is around 6.6 σ.

For comparison of different configurations, we use the constant separation in the drift space as a figure of merit. For other parameters, in particular for different crossing angles and β^* we get a scaling as (1):

$$\frac{d}{d_0} = \frac{\alpha}{\alpha_0} \cdot \sqrt{\frac{\beta^*}{\beta_0^*}} \tag{2}$$

Therefore an increased β^* allows a larger beam separation with reduced long range beam-beam effects or, for constant separation, a reduced crossing angle, providing more mechanical aperture. Since larger β^* is foreseen for the commissioning of the LHC and to evaluate the potential gain, we have studied different version of the LHC optics with increased β^* from the nominal 0.55 m to 1 m and 2 m. The loss of luminosity is not important during the commissioning and early days of operation of the machine.
The loss of luminosity due to the finite crossing angle can be easily computed as:

$$\frac{\mathcal{L}}{\mathcal{L}_0} = \frac{1}{\sqrt{1 + (\frac{\sigma_s \cdot \alpha}{2\sigma})^2}} = \frac{1}{\sqrt{1 + (\frac{\sigma_s \cdot \alpha}{2\sqrt{\beta^* \cdot \epsilon}})^2}} \tag{3}$$

where σ_s is the r.m.s. bunch length (0.0755 m for the LHC [3]).
In Tab. 1 we summarize the number for the cases we have studied. Although the case with a crossing angle of $\pm$ 200 μrad is not possible due to aperture restrictions, we have included it for comparison.

1.2 Collisions at injection energy

In the very initial stages of the commissioning, it is proposed to collide the beams at injection energy of 450 GeV, i.e. without ramping to nominal collision energy. To simplify the operation, the β^* cannot be reduced to the values foreseen for the top energy. Since the beam emittance is larger at injection, the beams require an increased aperture and collisions with long range interactions are excluded, in particular since non-linear magnetic field errors at injection will be important. It is therefore proposed to operate and collide without parasitic encounters, which implies a reduced number of bunches, i.e. 43 or 156. This entails the following consequences:

- No crossing angle and increased β^*
- Lower bunch intensity
- Low luminosity

It is further proposed to avoid the β-squeeze as well as the energy ramp and in order to reach a useful luminosity, it is planned to inject at a slightly reduced β^*. Values of 6 m and 11 m have been discussed at the time of this study.

$\beta^*_{x,y}$ (m)	half crossing angle (μrad)	F	separation (σ)
0.55	$\pm$ 100.0	0.91	6.6
0.55	$\pm$ 142.5	0.83	9.4
0.55	$\pm$ 200.0	0.73	13.2
1.00	$\pm$ 140.0	0.90	12.5
1.00	$\pm$ 160.0	0.87	14.3
2.00	$\pm$ 80.0	0.98	10.1
2.00	$\pm$ 100.0	0.97	12.6
2.00	$\pm$ 120.0	0.96	15.1

Table 1: *Crossing angle and resulting luminosity reduction factor F for different β^*. The normalized separation in the drift space between the interactions point and the first focusing quadrupole is computed from (1).*

2 Conditions for tracking

In the first part of the study we evaluated the standard collision parameters but with different β^*. The configurations we have used can be summarized in the following:

- Optics version 6.5 [5] and collisions at 7 TeV
- Nominal number of bunches (2808 per beam)
- Standard crossing scheme, i.e. alternating crossing planes in the high luminosity interaction points 1 and 5
- Intensity per bunch $1.15 \cdot 10^{11}$ protons
- $\beta^* = 0.55$ m, 1 m and 2 m.
- No high order field errors (i.e. no triplet errors)

In the second part of this study, i.e for injection energy, we evaluated the dynamic aperture under modified conditions. Details are given in a later section.

2.1 Procedure

To evaluate the dynamic aperture we performed a scan of the horizontal tune between 0.300 and 0.330 with Q_x - Q_y = 0.01, i.e. the vertical tune followed the horizontal value with a constant split. As dynamic aperture we defined a particle loss (10^6 turns) and we also computed the chaotic border for comparison.

2.1.1 Parameter set

Since the stability further depends on the relative horizontal and vertical amplitudes, different angles in the x-y plane are tested. In this study we expect an important effect since the x-y symmetry is broken in some cases. We use angular steps of 5^o, i.e. 17 different angles in the x-y plane. For each set of amplitudes and angles the horizontal and vertical tunes are assigned and the particles are tracked through the elements of the machine.

2.1.2 Magnetic field errors

The magnetic field errors in the final focusing quadrupoles were set up according to the specifications in [3]. For all β^* a correction algorithm was applied to minimize their impact, assuming the errors have been measured and are known. Typically 20 (top energy) and 60 (injection) different sets (seeds) of the field errors are used for each case.

2.1.3 Scan of working point

In order to find the best working points, the particles are tracked for different tune values. The nominal working point of the LHC in collision is 64.31 and 59.32 in the horizontal and vertical planes. For the tune scan the horizontal tune was varied in steps of 0.001. The tune

difference of 0.01 between the horizontal and vertical tune was maintained, i.e. the scan was performed parallel to the diagonal in the working diagram.
For the collisions at injection we did not scan the tune but fixed the values at the standard settings, i.e. 64.28 and 59.31. The configuration for collisions should be as close as possible to the standard injection settings.

2.1.4 Computing resources

The LHC@HOME system [7], based on the Berkeley Open Infrastructure for Network Computing (BOINC) [9], was used for here as reported in a previous study [4]. This provides the necessary computing resources required for a tune scan.

3 Tracking results

3.1 Standard collision optics with $\beta^* = 0.55$ m

For the nominal optics with $\beta^* = 0.55$ m we have done a tune scan and during the tune scan computed the onset of chaos and the dynamic aperture via particle loss over 10^6 turns.
In addition to the nominal crossing angle of $\pm$ 142.5 μrad we have studied two more crossing angles, a smaller angle of $\pm$ 100 μrad and an increased angle of $\pm$ 200 μrad. The latter is not possible in the nominal LHC due to the aperture restrictions in the triplet magnets, but we expect information for the foreseen LHC luminosity upgrade.
In addition to the tune scan we show the corresponding amplitude detuning caused by the beam-beam effects in the form of a footprint. This gives at least a qualitative information on the strength of the beam-beam interaction. Changing the crossing angle and therefore the strength of the long range interactions, we can compare the effect on the detuning.

The footprint for the smallest crossing angle ($\beta^* = 0.55$ m, $\alpha = \pm$ 100 μrad) is shown in Fig. 1. The footprint in Fig. 1 is shown for rather small crossing angle, i.e. a separation between the two beams of not more than 4 σ inside the triplet magnets. Particles at large amplitudes experience therefore occasional quasi head-on interactions and the picture is slightly obscured.

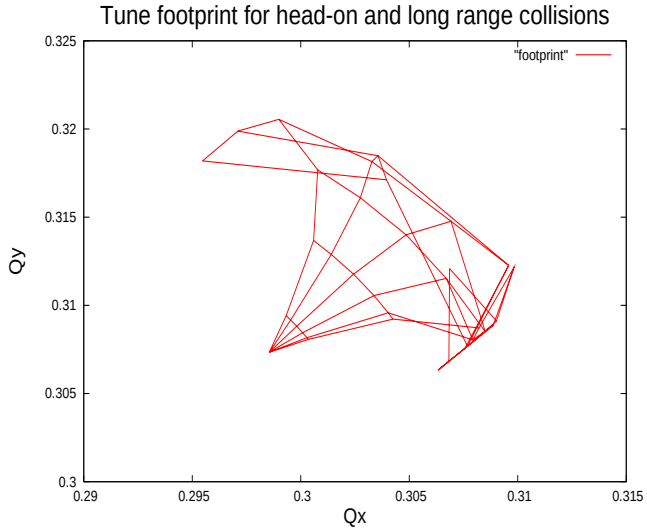

Figure 1: Tune footprint with head-on and long range beam-beam interactions. With $\beta^* = 0.55$ m. Crossing angle is $\pm$ 100 μrad.

Furthermore, it is expected that for $\beta^* = 0.55$ m the dynamic aperture is dominated by long range interactions. For a better comparison we have plotted in Fig. 2 footprints separately for the head-on contribution and the long range contributions for the three different angles. Since we expect the tune spread to decrease quadratically with the increased separation, the contribution of the long range interactions vanish rapidly for larger crossing angles Fig. 2. We expect significant differences in the dynamic aperture for the three cases.
Although the tune spread is a good indicator for the strength of the long range beam-beam

interactions, it is not the complete story. When the separation is large enough, i.e. above 10 σ, the large amplitude particles do not experience the most non-linear part of the beam-beam force from the opposing beam.

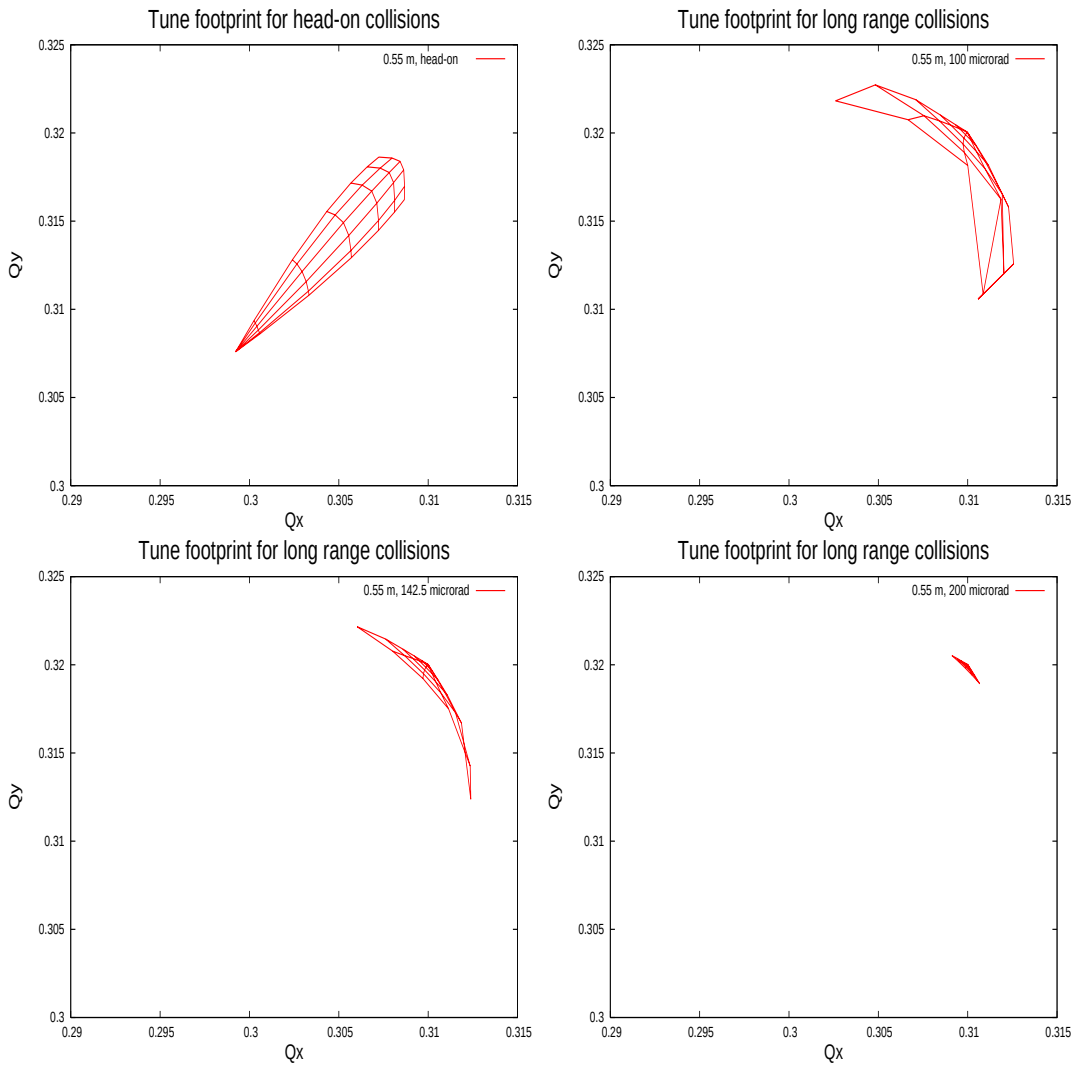

Figure 2: Tune footprint with head-on and long range beam-beam interactions. Top left for head-on only. Other pictures only long range interactions with crossing angles $\pm$ 100 μrad, $\pm$ 142.5 μrad and $\pm$ 200 μrad.

The results of the tune scan for the smallest angle are shown in Fig. 3. We have plotted

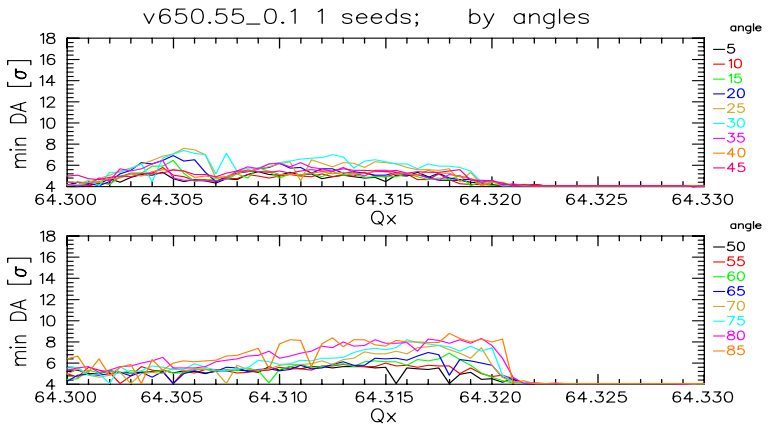

Figure 3: Tune scan: The dynamic aperture in units of the beam size is plotted as a function of the horizontal tune and for different angles in the x-y plane.With $\beta^* = 0.55$ m. crossing angle $\pm$ 100 μrad.

the minimum dynamic aperture as a function of the horizontal tune for different angles in the x-y plane. The dynamic aperture is small for the whole tune range covered by the scan. Obviously the beam separation at the long range encounters is insufficient. The effect of the third order resonance is clearly visible above fractional tunes of 0.320.

In the standard configuration with a crossing angle of $\pm$ 142.5 μrad the beam separation at the long range encounters is approximately 9.4 σ in the drift space between the interaction point and the first quadrupole magnet. The minimum separation inside the focusing triplet quadrupoles is $\approx$ 6.6 σ.
The Fig. 4 shows the tune scan for the nominal parameters. The results have been reported

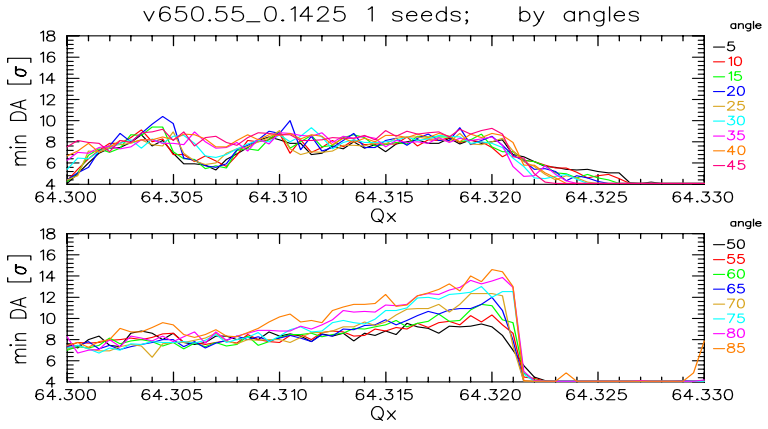

Figure 4: Tune scan: The dynamic aperture in units of the beam size is plotted as a function of the horizontal tune and for different angles in the x-y plane.With $\beta^* = 0.55$ m. crossing angle $\pm$ 142.5 μrad.

previously [4] and in the range of the nominal tune show a dynamic aperture above 8 σ for

all angles.

The tune scan for the large crossing angle of ± 200 μrad is shown in Fig. 5.

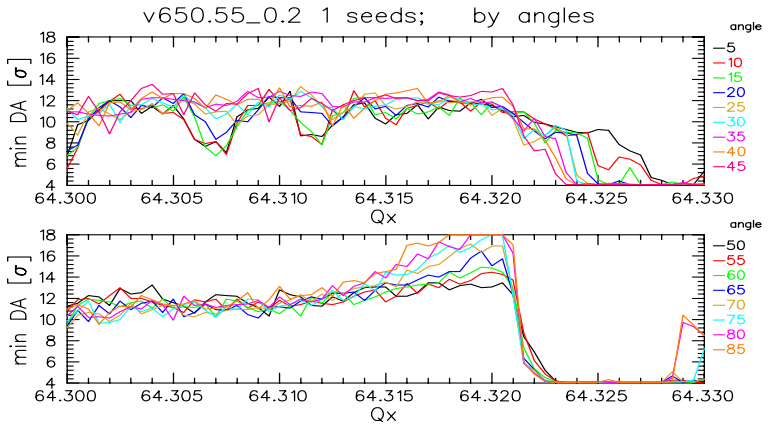

Figure 5: Tune scan: The dynamic aperture in units of the beam size is plotted as a function of the horizontal tune and for different angles in the x-y plane.With $\beta^* = 0.55$ m. Crossing angle ± 200 μrad.

The change of crossing angle is clearly visible in the detuning and is reflected in the dynamic aperture, a larger beam separation at the parasitic encounters improves significantly the dynamic aperture as expected. However an increase of the crossing angle for the nominal $\beta^* = 0.55$ m is difficult and limited by the mechanical aperture.
An increased beam separation can be achieved with a larger β^*. This is studied for two cases in the next section.

3.2 Collision optics with $\beta^* = 1.0$ m

The footprint for an increased β^* ($\beta^* = 1.0$ m, $\alpha = \pm 140$ μrad) is shown in Fig. 6. The

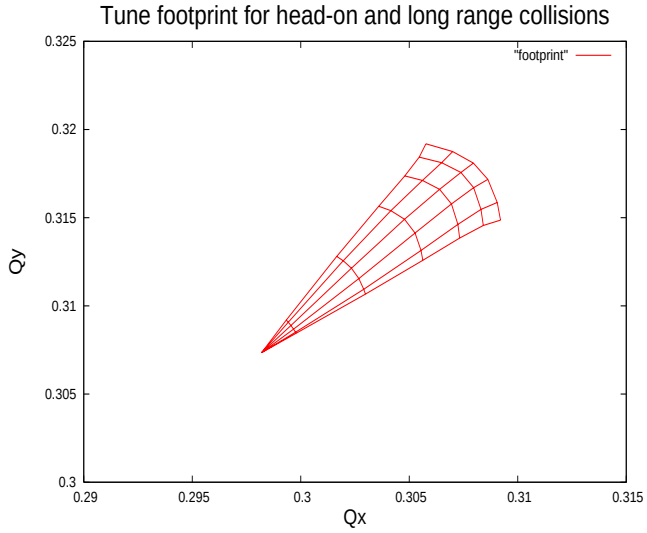

Figure 6: Tune footprint with head-on and long range beam-beam interactions. With $\beta^* = 1.0$ m. Crossing angle is $\pm$ 140 μrad.

required tune space is significantly smaller due to the reduced contribution of the long range interactions. The separation in the drift space is increased from 9.4 σ to 12.5 σ for the crossing angle of $\alpha = \pm 140$ μrad (see Tab. 1). The corresponding dynamic aperture for

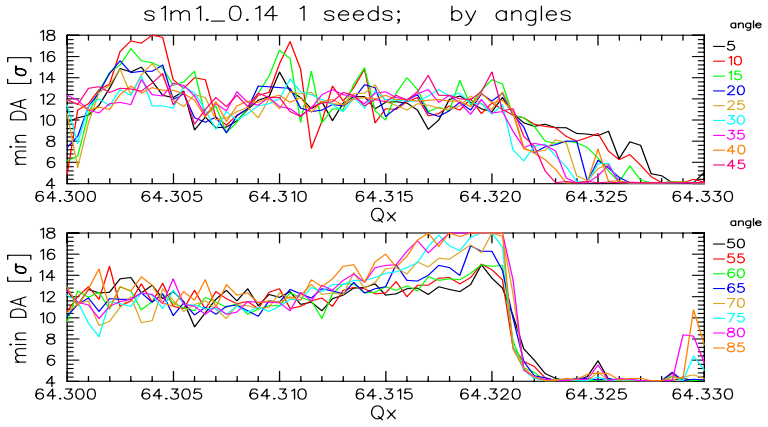

Figure 7: Tune scan: With $\beta^* = 1.0$ m. Crossing angle $\pm$ 140 μrad.

the different angles and as a function of the horizontal tune is shown in Fig. 7.

Compared to Figs. 4 and 5 the dynamic aperture is improved over the full range and in particular in the neighbourhood of the nominal tune the dynamic aperture is always above 8 σ.

The dynamic aperture can be further improved by an increased crossing angle. Due to the larger β^*, the geometric reduction factor as well as the aperture requirements are less

severe and permit this increase (see Tab. 1). The footprint for an increased crossing angle ($\beta^* = 1.0$ m, $\alpha = \pm 160$ μrad) is shown in Fig. 8. In this configuration the minimum

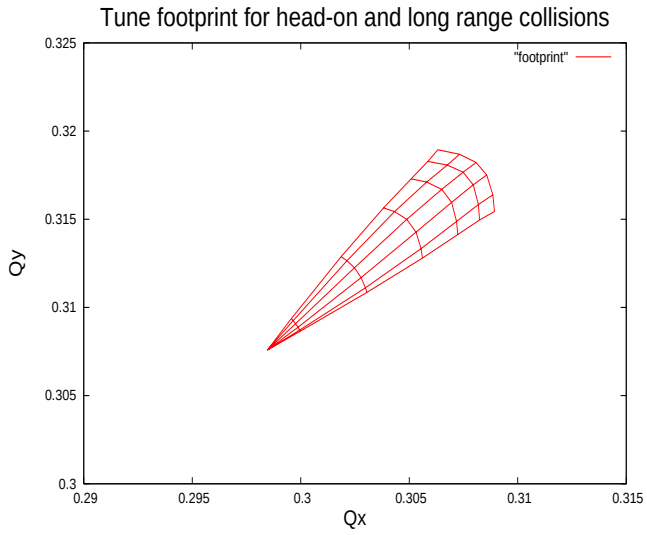

Figure 8: Tune footprint with head-on and long range beam-beam interactions. With $\beta^* = 1.0$ m. Crossing angle is $\pm$ 160 μrad.

separation between the two beams is always above 10 σ.

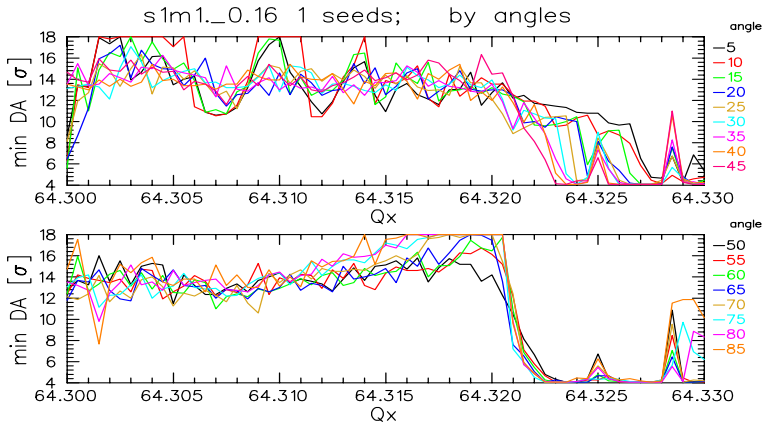

Figure 9: Tune scan: With $\beta^* = 1.0$ m. crossing angle $\pm$ 160 μrad.

The dynamic aperture with a crossing angle $\pm$ 160 μrad is shown in Fig. 9 and shows aperture well above 10 σ for all angles and tunes in the neighbourhood of the nominal working point. With this configuration no problems should be expected.

3.3 Collision optics with $\beta^* = 2.0$ m

In case of problems and for the initial commissioning phase a larger β^* of 2 m is foreseen and we have also evaluated this case for three different, possible crossing angles. The footprint for $\beta^* = 2.0$ m and a crossing angle of $\alpha = \pm 80$ μrad is shown in Fig. 10. The corresponding

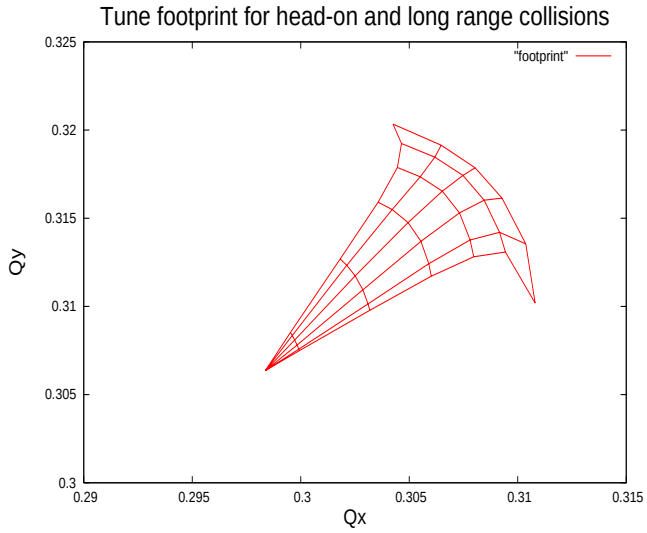

Figure 10: Tune footprint with head-on and long range beam-beam interactions. With $\beta^* = 2.0$ m. Crossing angle is $\pm$ 80 μrad.

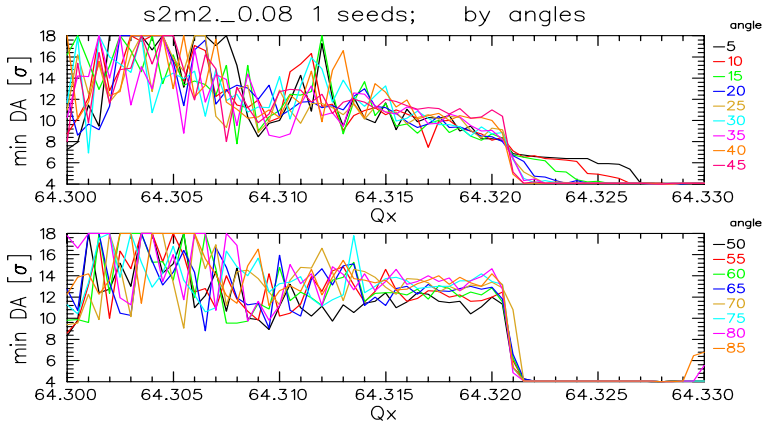

Figure 11: Tune scan: With $\beta^* = 2.0$ m. crossing angle $\pm$ 80 μrad.

tune scan (Fig. 11) for the rather small angle of $\pm$ 80 μrad shows sufficient dynamic aperture above 8 σ for all angles.

Increasing the crossing angle further should increase the available aperture again. The footprint for an increased crossing angle ($\beta^* = 2.0$ m, $\alpha = \pm 100$ μrad) is shown in Fig. 12.

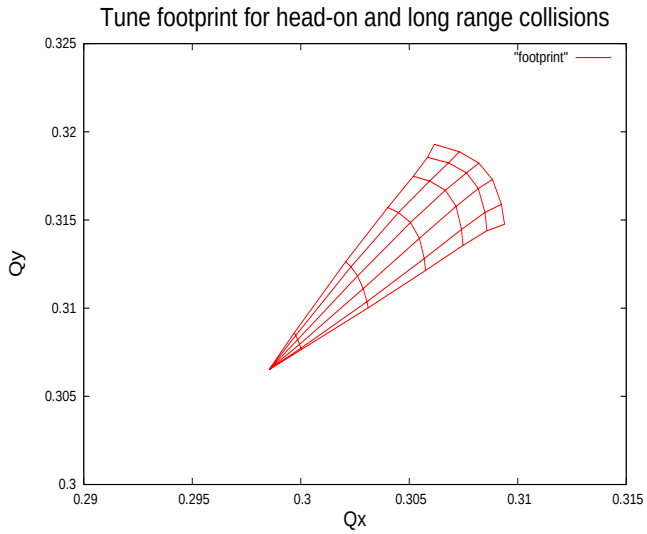

Figure 12: Tune footprint with head-on and long range beam-beam interactions. With $\beta^* = 2.0$ m. Crossing angle is $\pm$ 100 μrad.

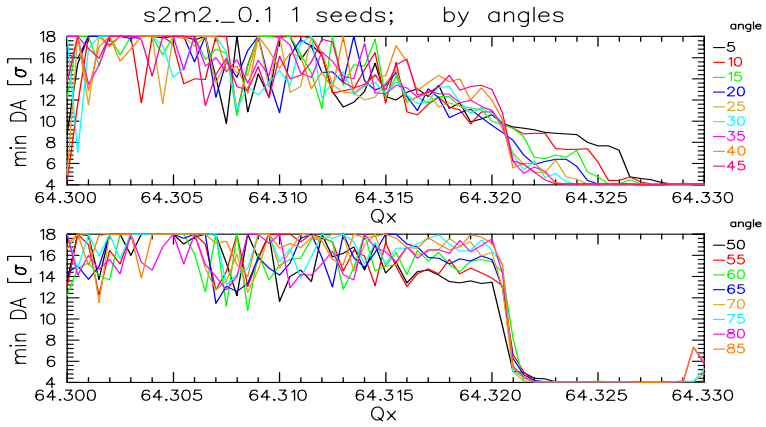

Figure 13: Tune scan: With $\beta^* = 2.0$ m. crossing angle $\pm$ 100 μrad.

Finally we have employed a crossing angle of $\alpha = \pm 120$ μrad. The footprint for this crossing angle ($\beta^* = 2.0$ m, $\alpha = \pm 120$ μrad) is shown in Fig. 14. The minimum separation is always larger than $\approx$ 12 σ, resulting in the small detuning from long range beam-beam interactions shown in Fig. 14. Almost the entire detuning is due to the head-on interactions.

The dynamic aperture with this parameter set is above 14 σ and safe for operation of the LHC.

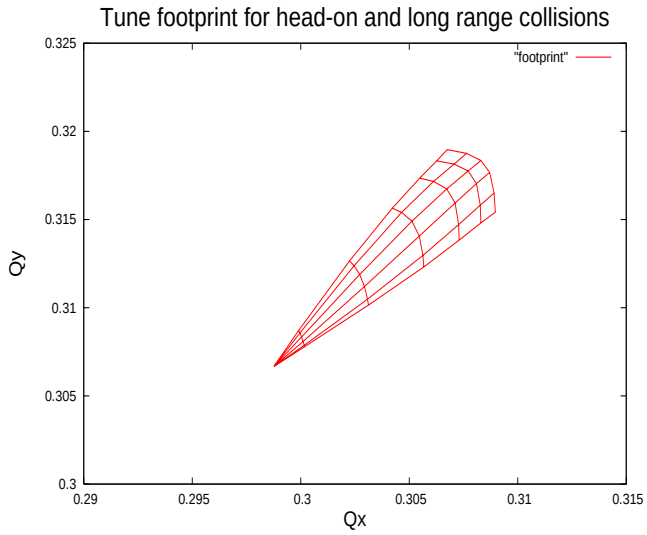

Figure 14: Tune footprint with head-on and long range beam-beam interactions. With $\beta^* = 2.0$ m. Crossing angle is $\pm$ 120 μrad.

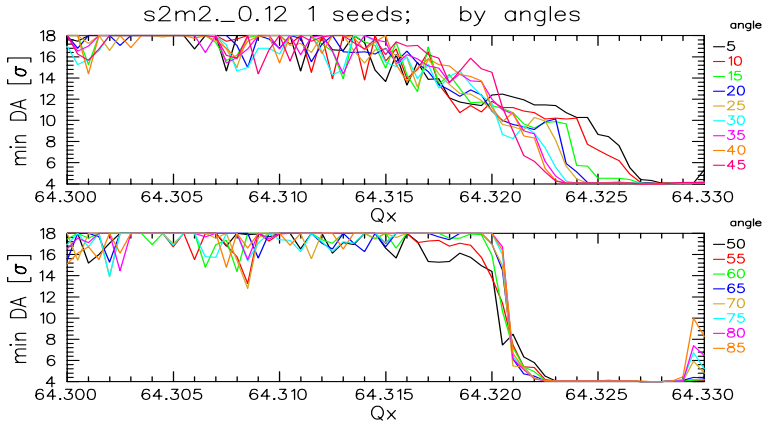

Figure 15: Tune scan: With $\beta^* = 2.0$ m. crossing angle $\pm$ 120 μrad.

4 Collisions at injection energy of 450 GeV

4.1 Conditions for tracking

To study the dynamic aperture with collisions at injection energy, we have used the following configurations:

- Injection optics version 6.5 with tunes 64.28 and 59.31.
- Maximum 43 to 156 bunches: no long range encounters[1]
- Intensity per bunch $0.4 \cdot 10^{11}$ protons
- $\beta^* = 6$ m, 11 m, and 17 m.
- High order field errors [8].
- Coupling due to a2 with and without correction.

The small number of bunches allow to operate without a crossing angle since no parasitic encounters can occur where the two beams share a vacuum chamber. Therefore only head-on collisions are simulated together with higher order field errors and coupling. It is well known that head-on collisions alone do not show any reduction of the dynamic aperture, however in the presence of other errors a significant effect is observed. This is true for the reduced bunch intensity of $0.4 \cdot 10^{11}$ protons per bunch,

[1] Since there will not be any long range encounters, the exact number of bunches is irrelevant in this study.

4.2 Collisions with $\beta^* = 17.0$ m

As the first case we have used $\beta^* = 17.0$ m which at the time of this study was the standard optics for injection.
In Fig. 16 we show the average (black crosses) and minimum (red squares) dynamic aperture for $\beta^* = 17.0$ m and 60 seeds for the field errors. The coupling due to the a2 field error are included and corrected. In this figure the head-on beam-beam effect is switched off for comparison. The simulation was done for eight angles in the x-y plane. The minimum dynamic aperture found in this case is above 10 σ. The Fig. 17 shows the results of a simulation

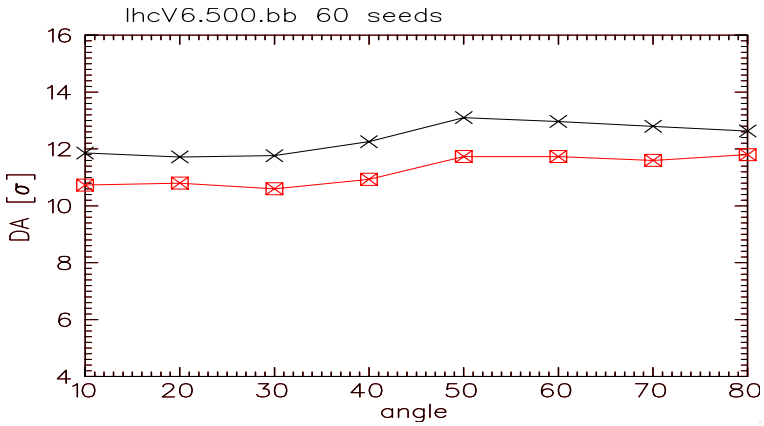

Figure 16: Average (black crosses) and minimum (red squares) dynamic aperture as function of angle in x-y plane. With $\beta^* = 17$ m. No crossing angle. Head-on beam-beam interactions switched off.

where the head-on beam-beam interactions are switched on. Otherwise the conditions are the same as in Fig. 16. A clear reduction of the dynamic aperture is observed and it can get

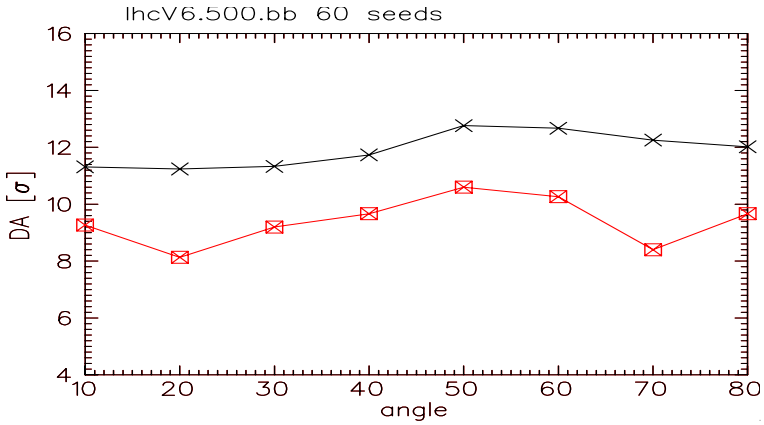

Figure 17: Average (black crosses) and minimum (red squares) dynamic aperture as function of angle in x-y plane. With $\beta^* = 17$ m. No crossing angle. Head-on beam-beam interaction on.

as small as 8 σ.

4.3 Collisions with $\beta^* = 6.0$ m

To obtain higher luminosity for collisions at 450 GeV a $\beta^* = 6.0$ m can be used. The simulation results for all errors together with the beam-beam interaction are shown in Fig. 18. The minimum is found around 7 σ together with a significant dependence on the angle on

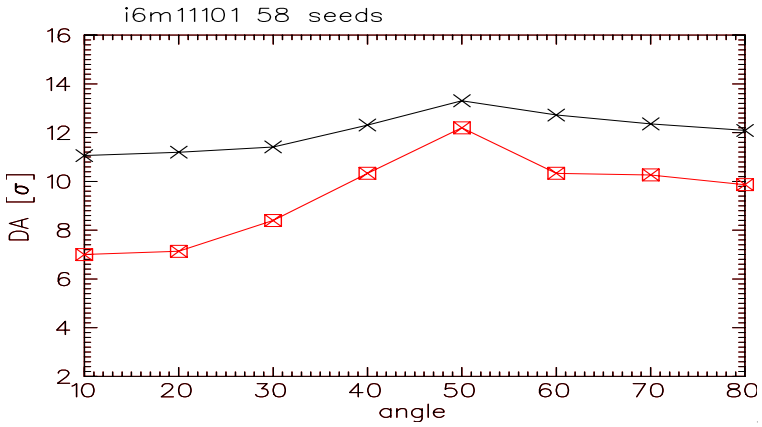

Figure 18: Average (black crosses) and minimum (red squares) dynamic aperture as function of angle in x-y plane. With $\beta^* = 6$ m. No crossing angle. Field errors, coupling and head-on beam-beam interaction.

the x-y plane. For comparison we show the results with the same conditions as above, except

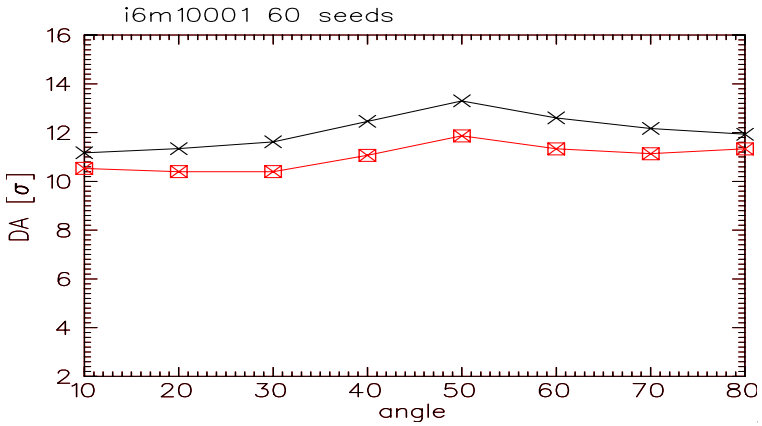

Figure 19: Average (black crosses) and minimum (red squares) dynamic aperture as function of angle in x-y plane. With $\beta^* = 6$ m. No crossing angle. Field errors and head-on beam-beam interaction, but no coupling.

that the coupling is switched off. A significant increase of the minimum dynamic aperture is observed, indicating the importance of the coupling in the presence of the beam-beam interaction. A significant difference of the average dynamic aperture is not seen, the low value of the dynamic aperture in the presence of coupling shown in Fig. 18 is caused by a single seed.

For comparison, we show in Fig. 20 the dynamic aperture for beam-beam interactions only, i.e. without field errors and without coupling. As anticipated, without any additional

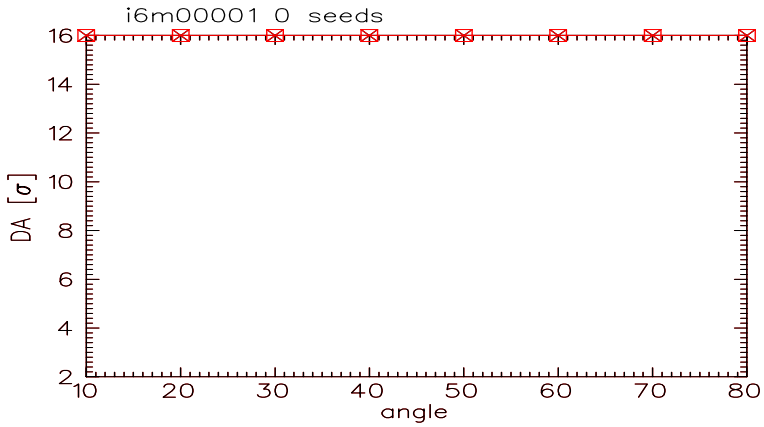

Figure 20: Average (black crosses) and minimum (red squares) dynamic aperture as function of angle in x-y plane. With $\beta^* = 6$ m. No crossing angle, beam-beam only, no field errors or coupling.

non-linear errors or coupling the head-on beam-beam effect does not reduce the dynamic aperture.

4.4 Collisions with $\beta^* = 11.0$ m

An alternative β^* for collisions at injection energy is $\beta^* = 11.0$ m and the results for the dynamic aperture are shown in Fig. 21. Higher order field errors and coupling are included. For all angles the aperture is larger than 10 σ

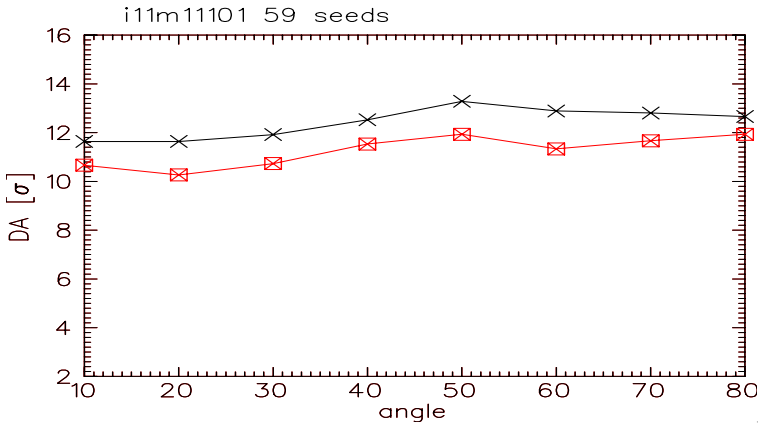

Figure 21: Average (black crosses) and minimum (red squares) dynamic aperture as function of angle in x-y plane. With $\beta^* = 11$ m. No crossing angle.

5 Summary

5.1 Collisions at top energy

In Tab. 2 we summarize the number for the cases we have studied for top energy. We repeat Tab. 1 and add the minimum dynamic aperture found in each case around the nominal working point. It is demonstrated that an increase of β^* is a very efficient way to increase

$\beta^*_{x,y}$ (m)	half crossing angle (μrad)	F	separation (σ)	dynamic aperture (σ)
0.55	$\pm$ 100.0	0.91	6.6	4.0
0.55	$\pm$ 142.5	0.83	9.4	7.0
0.55	$\pm$ 200.0	0.73	13.2	9.5
1.00	$\pm$ 140.0	0.90	12.5	9.0
1.00	$\pm$ 160.0	0.87	14.3	10.0
2.00	$\pm$ 80.0	0.98	10.1	8.0
2.00	$\pm$ 100.0	0.97	12.6	10.0
2.00	$\pm$ 120.0	0.96	15.1	12.0

Table 2: *Crossing angle and resulting luminosity reduction factor F for different β^*. The dynamic aperture is given in units of the beam size. The normalized separation in the drift space between the interactions point and the first focusing quadrupole is computed from (1).*

the dynamic aperture in case of problems due to long range beam-beam interactions. The loss of luminosity is moderate and acceptable for the commissioning phase and early operation. Even a relatively small increase of β^* can significantly reduce the long range effects, in particular since this also allows an increase of the crossing angle without additional aperture requirements or significant loss of luminosity.

5.2 Collisions at injection energy

We have evaluated the dynamic aperture for collisions at injection energy for three different β^* and can summarize as follows:

- Head-on beam-beam interactions alone do not cause particle losses for the reduced intensity.
- Including field errors and coupling we find a reduced **minimum** dynamic aperture:
  - For $\beta^* = 17$ m: dynamic aperture is 8 σ
  - For $\beta^* = 11$ m: dynamic aperture is 10 σ
  - For $\beta^* = 6$ m: dynamic aperture is 7 σ, depending on angle in x-y plane
- The **average** dynamic aperture however shows very similar behaviour for all β^* and we therefore cannot conclude a trend of the dynamic aperture as a function of β^*.

We conclude that collisions at injection energy are possible with an acceptable dynamic aperture.

References

[1] LHC beam-beam studies, http://cern.ch/lhc-beam-beam/

[2] W. Herr, *Features and implications of different LHC crossing schemes*, LHC Project Report 628 (2003).

[3] LHC Design Report, CERN-2004-003, (2004).

[4] W. Herr, E. McIntosh and F. Schmidt, CERN, D. Kaltchev, TRIUMF, Vancouver, Canada, *Large Scale Beam-beam Simulations for the CERN LHC Using Distributed Computing* Proc. EPAC 2006, Edinburgh 2006 (2006), page 528.

[5] T. Risselada, ABP-LCU section meeting, 29.01.2007.

[6] D. Kaltchev, ABP-LCU section meeting, 4.06.2007.

[7] "LHC@Home", http://lhcathome.cern.ch/.

[8] M. Giovannozzi, tracking sample job, private communication (2006).

[9] "BOINC: Berkeley Open Infrastructure for Network Computing", http://boinc.berkeley.edu/.

[10] D. Kaltchev, *On beam-beam resonances observed in LHC tracking*, TRI-DN-07-9, TRIUMF, 2007.